Official Dental Journal of Suez Canal University
DENTAL SCIENCE Updates
Print ISSN 2636-3836
Online ISSN 2636-3844
www.dsujournals.ekb.eg
DSU — Vol. 4, No. 1, March (2023) — PP. 65:76

STUDY THE POTENTIAL IMPACTS OF CHRONIC ORAL ADMINISTRATION OF SILVER NANOPARTICLES ON THE LINGUAL MUCOUS MEMBRANE AND SALIVARY GLANDS OF ALBINO RATS

Fatma Salem Soliman[1], Laila Sadek Ghali[2], Mervat Mohamed Youssef [3], Enas Mahmoud Hegazy[4]

DOI: 10.21608/dsu.2023.131153.1121
Manuscript ID: DSU-2204-1121

KEYWORDS

Albino Rats – Silver nanoparticles – Histological examination – Recovery – Tongue papillae- Toxicity

- E-mail address: dentist_fatma.salem88@yahoo.com.

1. Post graduate student at Oral Biology Department, Faculty of Dentistry, Suez Canal University.
2. Professor of Oral Biology, Faculty of Oral and Dental Medicine, Cairo University.
3. Associate Professor, Oral Biology Department, Faculty of Dentistry, Suez Canal University.
4. Associate Professor, Oral Biology Department, Faculty of Dentistry, Suez Canal University.

ABSTRACT

Introduction: The potential toxicity of silver nanoparticles (AgNPs) is becoming a more serious problem as interest in their uses in biotechnology and physiological effects grows. The toxicity of AgNPs was found to be dose and size dependent. **Silver nanoparticles synthesis:** Different routes lead to variable sizes, shapes, morphology, and even stability. Generally, these methods can be classified into three broad categories: physical, chemical, and biological (or green) synthesis. **Aim:** The aim of this work was to study the impact of oral administration of AgNPs on the mucous membrane and salivary glands of the tongue of albino rats. **Material and Methods:** Forty-six male albino rats were used in the present investigation. They were divided into the following groups: Group (1) (15 rats) they received 10mg/kg body weight AgNPs solution using curved metallic oro-pharyngeal tube for 21 days. Group (2) (15 rats) they were treated the same way as group 1 for 21 days then left for 1 month as a recovery period. Group (3) (16 rats) served as controls, subdivided into subgroup (3.1) (8) they received deionized water for 21 days. Subgroup (3.2) (8) they were treated the same way as subgroup 3.1 and then left untreated for one more month. Samples were examined under the light microscope for histological and immunohistochemical evaluation through PCNA labeling index where the number of PCNA positive cells were divided by the total cell number in the basal cell layer was estimated and treated statistically. **Results:** Examination of the tongue of the rats which were exposed to AgNPs solution revealed atrophic and degenerative changes of both the dorsal and ventral surfaces of the tongue as well as the lingual salivary glands. The examined tongues of the rats which were allowed a recovery period showed improvement in the histological picture. There was significant decrease in PCNA labeling index of the dorsal surface of the tongue of AgNPs treated group animals compared with control group as well as significant increase in PCNA labeling index of recovery group. **Conclusion:** Overexposure to AgNPs results in atrophic and degenerative effects. A one-month recuperation period can result in regeneration and an improvement in the histological appearance.

INTRODUCTION

Nanotechnology is manipulation of matter on an atomic, molecular, and supramolecular scale. The earliest, widespread description of nanotechnology referred to the particular technological goal of precisely manipulating atoms and molecules for fabrication of macroscale products, also now referred to as molecular nanotechnology [(1)].

One of the most researched nanomaterials is silver nanoparticles (AgNPs(. They have specific surface area of several hundred m2/g. Their unique surface features endow AgNPs with a unique set of physicochemical properties not found in solid materials [2].

The fact that silver ions are hazardous to microbiological agents that have been successfully implemented in research. AgNPs formulation will improve a wide range of antibacterial characteristics due to the massive increase in surface area in nanoparticles formulation. Furthermore, these antibacterial effects have been demonstrated against bacteria that are resistant to antibiotics [3]. Despite their efficacy in a variety of medical applications, AgNPs remain a contentious study topic in terms of their toxicity in biological and ecological systems[4].

Although the use of AgNPs in new applications continues to grow, the toxicity them in biological systems remains disputed. The oral toxicity of AgNPs, may have potential toxicity at certain doses and can cause a variety of health concerns if utilized incorrectly [5].

The harmful effect of AgNps can pass through the biological membranes and even extremely small capillaries throughout the body (e.g., the blood-brain (BBB) and blood-testes (BTB) barriers. Nanoparticle toxicity is known to be influenced by their size, shape, and surface area[6,7]. Silver nanoparticles have the potential to produce chromosomal abnormalities and DNA damage, as well as growth arrest in cell lines, according to in vitro and in vivo toxicity studies [8-10].

The rate of epithelium activity is determined by immunohistochemical detection of the proliferative cell nuclear antigen (PCNA(. As a result, it can be used as a monitor to see how AgNPs affect epithelial cells. In this regard, human and animal studies are very limited, more researches are needed before final conclusions. The evidence for AgNPs' carcinogenicity in humans is insufficient, but there is some evidence in experimental animals and in vitro research [11,12].

MATERIAL AND METHODS

Preparation and characterization of the silver nanoparticles:

Rapid green method)13(. was used for preparation and characterization of AgNPs. Pomegranate fruits were collected from the local market. Siver nitrate ($AgNO_3$ > 99.9%) and chloroauric acid*1 (> 99.9%) was obtained from International Company for Scientific and Medical Supply. All glassware and pome fruit were properly washed with deionized water and were dried in oven. Fruit peel extract (FPE) of pome were used as a reducing agent for the development of AgNPs.

Properly washed 50g of fresh peels of the fruit were added in 250ml ultra-pure water in 500ml Erlenmeyer flask and boiled for 10-15 minutes. Whatman filter paper (No. 40) was used for filtration of boiled material to prepare an aqueous fruit peel extract, which was used as such for metal nanoparticle synthesis.

Aqueous silver nitrate chloroauric acid solution (1mM) was generated 50ml of the metal (Ag) ion solution was reduced for 5 minutes at room temperature using 1.8ml of FPE. The solution took more than 10 minutes to achieve a significant surface plasmon resonance (SPR) for the metal nanoparticle below this fruit peel extract level.

Experimental Design

This study was approved by the ethical committee of Faculty of Dentistry Suez Canal University; No 121/2018.

The sample size was calculated using the following formula using a confidence level of 95% and confidence interval of 2.5.

$$\text{Sample size} = \frac{z^2 * (P) * (1-p)}{c^2}$$

Where:

*Z=z value

*P=proportion of the population having the attribute

*C=Confidence interval, expressed as decimal.

So, by calculation, the sample size was equal to 15 animals per group, giving a total sample size of 46 animals.

Forty-six adult male albino rats with an average 150-180 gm / kg were used. They were divided into the following groups:

- **Group 1:** 15 rats; were given 10 mg/kg day AgNP solution (3 to 20 nm) [14] via a curved metallic oro-pharyngeal tube for 21 days.
- **Group 2**: 15 rats; were given the same treatment as group 1 for 21 days before being given a month to recover.
- **Group 3:** 16 rats; served as controls, receiving deionized and subdivided into the following categories:

Subgroup 3.1 8 rats; received deionized water for 21 days.

Subgroup 3.2 8 rats; were treated the same way as subgroup 3.1 and then left untreated for one more month.

The animals in each group were euthanized by cervical dislocation at the end of the experiment, their tongues were dissected, fixed in 10% neutral buffered formalin, processed, and embedded in paraffin. 5μ sections were stained using Haematoxylin and Eosin (H&E) stain to detect histological changes.

Preparation of Specimen for PCNA immunohistochemical detection:

Other 5μ sections were cut from paraffin blocks and mounted on positively charged slides. Then, they were preincubated in absolute methanol to block any endogenous peroxidase activity without affecting the immunoreactivity of the antigen. After a gentle rinsing with phosphate buffer solution, the sections were incubated with non-immune sera for 10 minutes (Reagent 1A). Each portion received two drops (equal to 100l) of primary antibody, which was kept on for 30-60 minutes. PBS was used to rinse the sections three times for two minutes each time. Excess buffer was removed from the slides, and they were wiped clean. Each portion received two drops of biotinylated second antibody (Reagent 1B) containing antimouse antibody, which was incubated for 10 minutes. The pieces were then washed in three different concentrations of PBS for two minutes each.

Primary Antibody; Name: PCNA antibody, Clone: PC-10, Mouse anti-Rat, Supplier: Santa Cruz Biotechnology, Catalog Number: sc-56, Dilution: 1:2000 using IHC-TekTM Antibody Diluent (Cat# IW-1000 or IW-1001) to reduce background and unspecific staining and serum blocking step is NOT needed and Incubation Time/Temp: 60 min/ room temperature. Antigen Retrieval; Device: IHC-TekTM Epitope Retrieval Steamer Set (Cat# IW-1102), Buffer/pH value: IHC-TekTM Epitope Retrieval Solution (Cat# IW-1100), Heat/Cool Temperature: 95-100 ºC/room temperature and Heat/Cool Time: 20 minutes/20 minutes.

After that, hematoxylin was used to counterstain the sections. The PCNA labelling index (the number

of PCNA positive cells divided by the total cell population in the basal cell layer) was calculated and treated statistically after the slides were inspected under a light microscope. Immunopositive staining was defined as any nuclear staining, regardless of intensity.

Preparation of the specimen for examination by scanning electron microscopy:

Other representative tongue specimens were fixed in 2.5 percent glutraldhyde in 0.1M phosphate buffer (PH 7.4) for 4 hours in all groups of rats. The samples were then rinsed with phosphate buffer and post-fixed for 90 minutes in 1 percent osmium tetroxide, after which they were washed again with phosphate buffer and dehydrated through a sequence of escalating ethanol concentrations to 100% amylacetate)14(.

After that, samples were coated with gold under vaccum with sputter coater. After gold coating, tongue samples were examined and photographed with JEOL, JSM-53009 scanning electron microscope in EM unit, Central Laboratories Sector, The Egyptian Mineral Resources Authority, Cairo.

RESULTS

I. Histological Results: (Haematoxylin and Eosin stain)

The histological examination of hematoxylin and eosin-stained sections of the mucous membrane of the tongue of the control rats showed the normal histological features of surface epithelium and underlying lamina propria both in sub-groups 3.1 and 3.2. The filiform papillae (**fig. 1A**) had a sharp conical appearance and were coated in stratified squamous epithelium with a thin regular keratin coating. The fungiform papillae (**fig.1B**) were found in between the filliform papillae, which had a broader surface and a wider vascular connective tissue core and were most commonly seen near the tongue's tip and lateral borders. The single circumvallate papilla (**fig.1C**) was found near the V-shaped sulcus terminalis. There was a circular furrow all around it. Many taste buds were discovered in the papilla's side walls and furrows. The ventral surface of the tongue was covered with keratinized stratified squamous epithelium that sent numerous broad epithelial ridges towards the underlying lamina propria, the later was formed of loosely arranged collagen fibers in the papillary and dense collagen bundles in the reticular layers, in addition to the connective tissue cells, blood vessels and nerves (**fig.1D**). At the bottom of the furrow opened the ducts of pure serous salivary glands situated beneath the circumvallate papillae. They were formed of normal serous acini (**fig.1E**). And pure mucous salivary glands were also seen among the lingual muscle fibers posterior to the pure serous glands (**fig.1F**).

Examination of the tongues of rats which were exposed to AgNPs revealed atrophic and degenerative changes that involved the surface epithelium and lamina propria of both the dorsal and ventral surfaces of the tongue as well as the lingual salivary glands. The filiform papillae (**fig.2A**) lost the normal appearance. They were markedly atrophic; their number and height were apparently much decreased when compared with those of the control animals. Most of them appeared stunted with total or partial loss of their characteristic conical shape and evident hyperkeratosis. Their epithelial covering showed marked atrophy and the lamina propria showed signs of degeneration. The fungiform and circumvallate papillae showed signs of atrophy in their epithelium and lost their normal configuration (**fig.2B, 2C**). Taste buds appeared shrunken, partially lost their cells or completely absent. The mucous

membrane on the ventral surface of the tongue of rats exposed to AgNPs displayed severe atrophic and degenerative alterations, including a reduction in the thickness of the surface epithelium, dissociation of the lamina propria collagen fibres, and dilation of blood vessels (**fig.2D**). The lingual glands also suffered marked degenerative changes in the acinar and ductal cells of both the serous and mucous glands. The serous acinar cells presented marked intracytoplasmic vacuolizations that sometimes completely destroyed the whole cells. The mucous acinar cells were also seriously affected with a lot of cystic transformations of the acini and marked dilatation of the ducts (**fig.2E, 2F**).

The histological picture of the surface epithelium and lamina propria of the dorsal and ventral surfaces of their tongues, as well as their lingual salivary glands, improved in the studied tongues of the rats who were given a one-month recovery period following 21 days of oral administration of AgNPs. In compared to the AgNPs-treated group, the number and height of the filliform papillae increased (**fig.3A**). The fungiform and circumvallate papillae appeared to be in rather good condition, with no evidence of atrophy or degeneration. Their taste buds recovered and returned to a more or less normal state (**fig.3B, 3C**). The surface epithelium of the ventral surface of the tongues had normal thickness of surface epithelium, normal pattern of epithelial ridges with normal density of collagen fibers of its lamina propria (**fig.3D**). The serous and mucous acini of the lingual glands showed improvement of the histological architecture of their acini and ducts. There was total or subtotal absence of intracytoplasmic vacuolization in the serous acinar cells and nearly no cystic transformation in the mucous acinar cells or ducts (**fig.3E, 3F**).

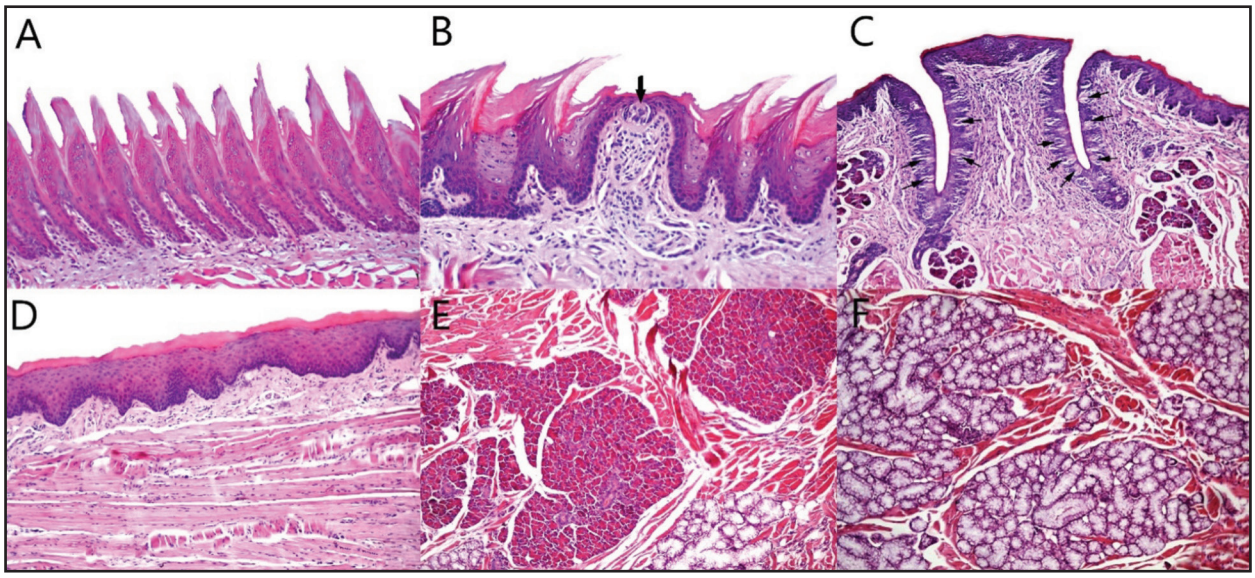

Fig. (1) Photomicrographs of the dorsal, ventral surface and lingual salivary glands of the control tongue showing: **A**-Sharp conical projections of filiform papillae with thin smooth keratinized epithelial covering and lamina propria. Skeletal muscle fibers running in different directions are seen underneath the papillae. **B**-A fungiform papilla with normal barrel like intraepithelial taste bud (arrow). **C**-A circumvallate papilla with a lot of taste buds at its side walls (arrows). **D-**The ventral surface of the tongue formed of surface epithelium and lamina propria. **E-**The pure serous gland with its small rounded acini lined with secretory cells having rounded basophilic nuclei at the basal third. **F-**The pure mucous gland with large lightly stained mucous acini (H&E, orig. mag. A-200, B-200, C-100, D-200, E-100, F-100).

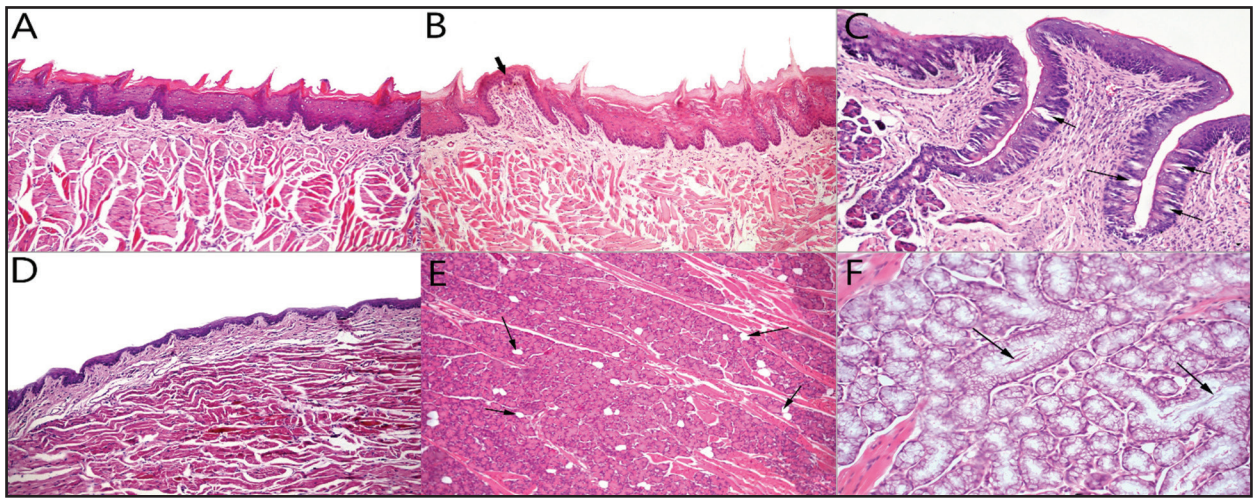

Fig. (2) A photomicrograph of the tongue of AgNPs treated group rats showing: **A**-Atrophy and apparent decrease in the height and number of filiform papillae. **B**-Fungiform papilla (among atrophic filiform papillae) with degenerated taste bud (arrow). **C**-Circumvallate papilla showing atrophy of the taste buds with degenerating cells (arrows) and collection of inflammatory cells in the lamina propria (small arrows). **D**-The ventral surface of the tongue of group 2 rats showing atrophy of the surface epithelium and dissociation of collagen fibers of the lamina propria **E-**The serous acinar cells showing degeneration with a lot of intracytoplasmic vacuolization (arrows). **F**- the tongue of AgNPs treated group rats showing cystic transformation of some of the mucous acini (arrows) (H&E, orig. mag. A-100, B-200, C-200, D-100, E-100, F-200).

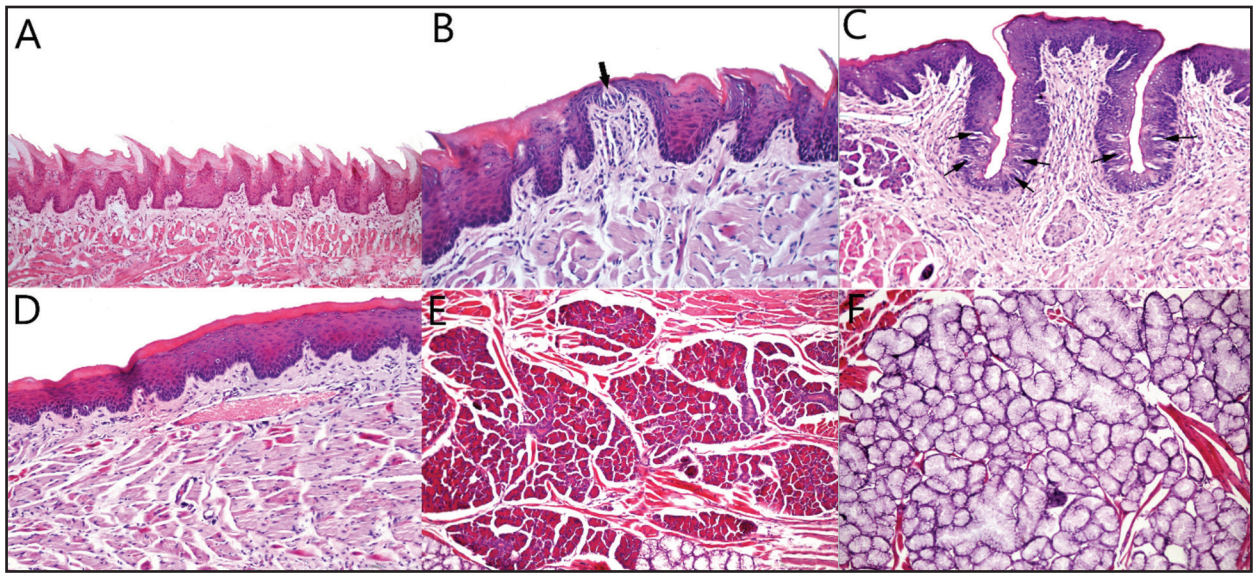

Fig. (3) Photomicrographs of the dorsal surface of the tongue of the recovery group rats showing: **A**-Sharp conical projections of filiform papillae with thin smooth keratinized epithelial covering and lamina propria. Skeletal muscle fibers running in different directions are seen underneath the papillae. **B**-A fungiform papilla with normal barrel like intraepithelial taste bud (arrow). **C**-A circumvallate papilla with a lot of taste buds at its side walls (arrows). **D**-The ventral surface of the tongue of recovery group rats showing normal epithelium covering and normal density of the collagen fibers of the lamina propria. **E-**The serous salivary gland of the tongue of recovery group rats showing total absence of intra-cytoplasmic vacuolization of the serous acinar cells. **F-**The mucous salivary gland of the tongue of recovery group rats showing nearly normal mucous acini with minimal cystic transformation (H&E, orig. mag. A-100, B-200, C-200, D-200, E-100, F-100).

II. Immunohistochemical results: (Proliferating Cell Nuclear Antigen (PCNA)

The histological sections of tongues of the controls revealed moderately to strongly positive PCNA staining reaction mainly at the basal and parabasal cells of the surface epithelium indicating normal proliferation of the cells of the dorsal and ventral surfaces of the tongue. All the basal cells were positively stained (**fig.4A**).

The basal layer of the epithelium of the dorsal and ventral surfaces of the tongue of rats exposed to AgNPs had low expression of PCNA, ranging from negative to weakly positive staining reaction, indicating a decrease in proliferation of basal and parabasal cell layers, indicating a marked decrease in the rate of turnover and cell renewal. The majority of the basal cells were stained negatively (**fig.4B, 4C**).

The sections of the tongues of rats allowed for recovery showed moderately to strongly positive PCNA expression in the basal and parabasal cells of the dorsal and ventral surfaces of the tongue (**fig.4D**).

Statistical analysis of PCNA immunostaining reaction: According to the results of kruskal-wallis test (table 1):

- Control group showed the highest mean value of PCNA immunoreactivity expression. The mean number of proliferating cells reached its maximumlevel (48.91± 5.66). While Nanosilver treated group revealed the lowest mean value (7.86± 2.72) of PCNA immunoreactivity.
- The mean number of immunopositively cells of recovery group (35.84±7.29), revealed that PCNA expression was less than thoseof control group, but without significant difference

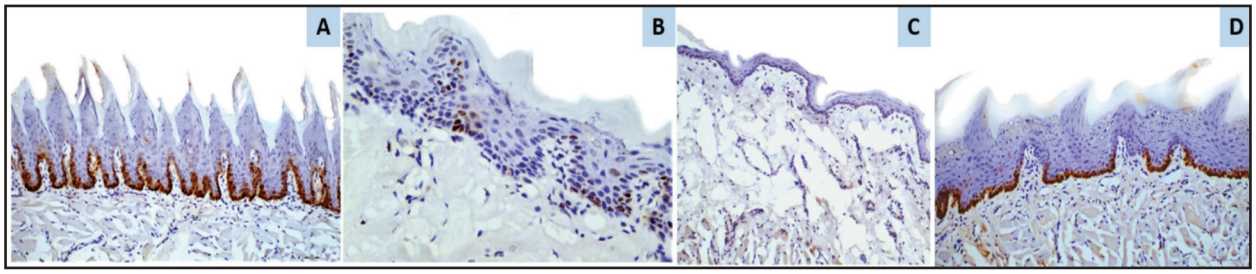

Fig. (4) A photomicrograph of the tongue showing: **A**-The dorsal surface of the tongue of control group 3.1 rats showing strongly positive PCNA staining of the basal cells of the epithelium of filiform papillae. **B**-The tongue of group 2 rats showing the dorsal surface with negative to weakly positive staining reaction of the basal cells to PCNA. **C**-The ventral surface of the tongue of AgNPs treated group rats showing negative to weakly positive staining reaction of the basal cells to PCNA. Most of the basal cells are negatively stained. **D**-The dorsal surface of the tongue of recovery group rats showing moderately to strongly positive PCNA staining of the basal. Almost all the basal cells are positively stained (orig.mag. A-200, B-400, C-200, D-200).

There was highly significant difference between the Nanosilver group and others, where the p value ≤ 0.00.

Table (1) *Showed the value number (mean ±SD) of PCNA immunopositively cells in the tongue of different studied groups.*

Groups	Mean±Std. Deviation	P-Value ≤0.05
Control	**48.91[a]± 5.66**	
Nanosilver treated	**7.86[b]± 2.72**	0.001**
Recovery	**35.84[a]±7.29**	

***;a.b; means significant differences between groups using Kruskal –Wallis test at (P value≤0.05) SD: Standard deviation*

III. Scanning Electron Microscopic results:

The dorsal surface of the tongues of control rats revealed numerous pointed conical filiform papillae with uniform keratinized tips grouped in parallel regular rows indicating a consistent antero-posterior orientation towards the tongue root. Among the numerous filiform papillae, there were scattered fungiform papillae with broad apices that were dome-shaped or mushroom-shaped and broader in diameter than the filliform ones. Around a centrally positioned well defined regular gustatory opening bordered by shallow depression, thin epithelial smooth cells were revealed. (**fig.5A**).

Numerous filiform papillae with clearly altered orientation and inclination were found on the dorsal surface of rats' tongues that had been

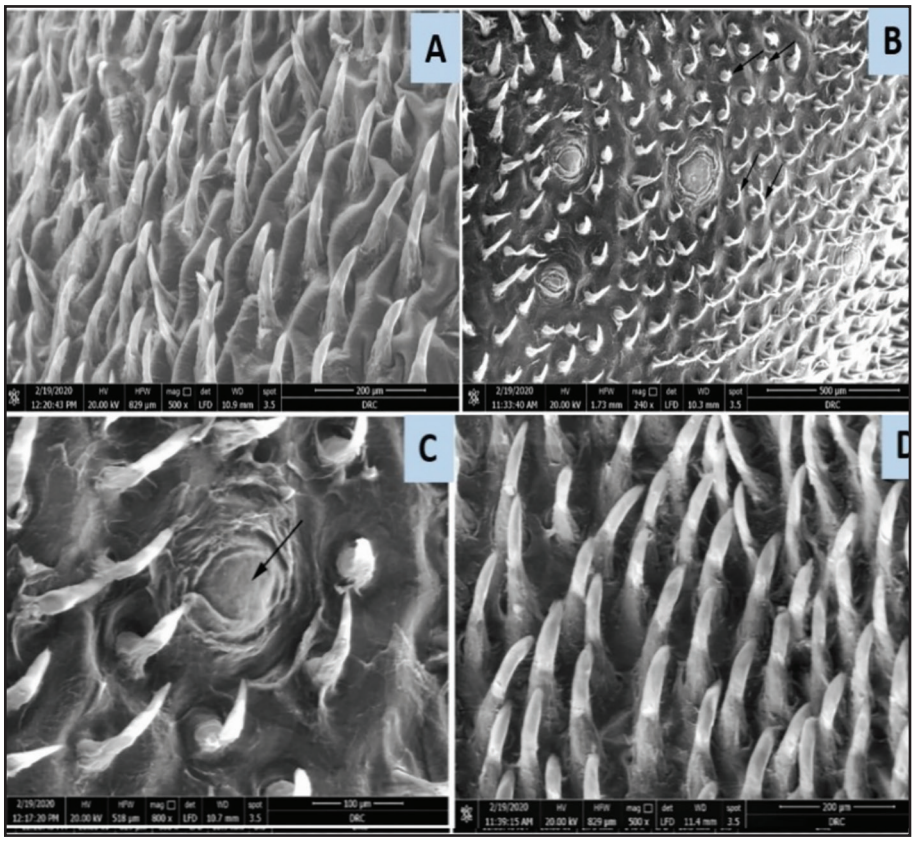

Fig. (5) Scanning electron micrograph showing: **A**-The dorsal surface of the tongue of control group rats showing regular parallel rows of long conical filiform papillae with tapering ends. **B**-The dorsal surface of the tongue of AgNPs treated group rats showing different distribution, extreme thinning and stunting of the filiform papillae. **C**-The dorsal surface of AgNPs treated group rat's tongue showing fungiform papilla with obliterated taste pore (arrow). **D**-The dorsal surface of the tongue of recovery group rats showing well developed filiform papillae with long conical shape (mag. A-X500, B-X240, C-X800, D-500).

exposed to AgNPs. They saw a noticeable fall in number as well as a shift in distribution. Filiform papillae degeneration resulted in stunted auxiliary processes surrounding the primary projection. They became thinner, with a narrow shape rather than a conical one, with anomalous severe bending or looping. Others had keratin that was restricted. Some filliform papillae had blunt eroded tips as well. (**fig.5B**). Fungiform papillae were portrayed with a wrinkled, strongly keratinized epithelial coating (**fig.5C**). They had shrunken, atrophied, and deteriorated in size. In the centre region at the top of each fungiform papilla, the tasting pore was frequently apparent. The gustatory pore might be depressed, irregular, ill-defined, or destroyed.

The examined tongues of the rats which were allowed a recovery period for one-month revealed almost normal direction and distribution of filiform papillae. However, some papillae still suffered signs of destruction. They were conical in shape and long. The filiform papillae were numerous in number covering the dorsal surface and extend to the lateral borders (**fig.5D**). The fungiform papillae were nearly typical in size and appearance, with well-defined taste buds. Taste holes and scaling cells were visible on the surface of the fungiform papillae.

DISCUSSION

The rats in this study were given 10 mg/kg body weight of AgNP solution orally every day as a toxic dose, which was the same as that found by **Shahare et al** [15]. The current findings revealed atrophic modifications in the lingual papillae of AgNPs exposed rats' tongues, manifested as atrophic filiform papillae with alterations in their usual height and number. They had a stunted look, with total or partial loss of their conical shape and evident hyperkeratosis. Their epithelial covering showed marked atrophy. The taste buds of fungiform papillae were altered through appearance of shrinkage and vacuolization of their cells, as well as a peripheral arrangement of the cells leaving an empty center. Others revealed total cell degeneration. **Sarhan and Hussein**)16(observed similar histological alterations in the renal cortex of rats intoxicated with AgNPs via intraperitoneal injection at a dose of 2,000 mg/kg for just 2 days, with inflated epithelium and cytoplasmic vacuolations, as well as hypertrophied nucleoli in some nuclei.

The circumvallate papillae were found to be severely affected in the current study; they lost their normal configuration, appeared atrophic, and displayed markedly degenerating taste buds, with their remaining cells surrounded by partially empty spaces and a shallowing or partial loss of the furrow surrounding the papillae. **Sarhan and Hussein**)16(found hepatocytes with severe cytoplasmic vacuolization, many intranuclear and intracytoplasmic fat globules of varied sizes, and fractured rough endoplasmic reticulum in the livers of albino rats after treatment of AgNPs. Mitochondria seemed enlarged, with packed electron-dense matrices and some cristae missing.

The lingual salivary glands showed significant degenerative alterations in the acinar and ductal cells of both the serous and mucous glands in the current study. Intracytoplasmic vacuolizations were seen in the serous acinar cells, which sometimes resulted in the entire death of the cells. Cystic changes also had a significant impact on mucous acinar cells. **Oberdorster**)17(found that several nanoparticles applied to human cells release free radicals within the biological system, causing oxidative stress, which leads to an increase in inflammation, cellular death, and genotoxicity.; Free radicals on the surface of nanoparticles can activate the redox cycle and produce toxicity in numerous cell components. Chemistry, surface, size, dose, and particle delivery

method all play a role in the harmful mechanism of nanoparticles in organisms. **Asharni et al**)18(addressed these findings by stating that AgNPs can damage DNA and produce chromosomal abnormalities. Indirectly, this damage was induced by an increase in reactive oxygen species (ROS) production or a decrease in ATP synthesis, which resulted in mitochondrial damage, impairing energy-dependent DNA repair mechanisms.

The size of the silver nanoparticles used in our study ranges from 3 to 20 nm, which matches the findings of **Osborne et al**)19(who found that the amount of damage caused increased as the nanoparticle size decreased because they were able to cross the basement membrane and accumulate in body tissues. The largest levels of accumulated AgNPs are seen in the liver, spleen, gut, stomach, and heart.

In our study the underlying lamina propria showed degeneration and dissociation of collagen fibers with marked dilatation of blood vessels and their engorgement with blood cells. Occasional inflammatory cells infiltration was seen in the lamina propria of the tongues of rats treated with AgNPs. Similar findings were reported by **Freed and Gutterman**)20(through the mitochondrial ROS-dependent and -independent mechanisms, mitochondrial membrane depolarization produces endothelium-derived relaxing factors including NO which investigated tissue perfusion.

The immunohisto- chemical detection of the (PCNA) that indicates the rate of cell activity of the epithelium of rats treated with AgNPs. The stained sections showed little or no staining with PCNA in the basal cell layer of the tongue epithelium of rats exposed to AgNPs while those of the controls presented strongly positive reaction indicating marked decrease in the rate of turnover and cell renewal of the treated rats. These findings are consistent with those of **Cortese- krott**)21(who found that AgNPs cause pro-inflammatory cytokines to be produced in the cells, resulting in a large number of free radicals and increased expression of the NOX/NADPH oxidase family, which causes DNA damage, cell death, and apoptosis. Overproduction of ROS and activation of oxidizing enzymes, according to **Cayli et al**)22(resulted in cytoskeletal, cell membrane, and mitochondrial damage, as well as germ cell specific apoptosis.

AgNPs can also damages cell membranes and promote apoptosis by oxidative damage, according to **Cheng et al.**)23(Damage to fibroblast membranes allows calcium to enter the cell, causing intracellular calcium excess, as well as increased production of (ROS) and changes in mitochondrial membrane potential. These particles can pass cell membranes and cause cell harm, according to **Hussain et al.**)24(

In the present investigation the tongues of the rats which were allowed a recovery period for one-month after 21 days of AgNPs administration showed improvement in the histological picture of the surface epithelium and lamina propria of the dorsal and ventral surfaces of their tongues as well as their lingual salivary glands. The filiform papillae showed an apparent increase in their number and height. The fungiform and circumvallate papillae appeared more or less normal without signs of shrinkage or degeneration. Their taste buds got regenerated and appeared more or less normal. The surface epithelium of all types of papillae showed marked increase in thickness and length of their epithelial ridges. The serous and mucous acini of the lingual glands showed improvement of the histological architecture of their acini and ducts. There was total or subtotal absence of intracytoplasmic vacuolization in the serous acinar cells and nearly no cystic transformation in the mucous acinar cells or ducts.

Rung by et al)25(found that 0.015% silver nitrate in the drinking water for 125 days (14 mg/kg of bw/day) induced hypoactivity in mice after a 10 day silver withdrawal period. An increase in liveliness was noticed in rats fed 0.01 percent silver nitrate in their drinking water for four months, according to another study. In a research by **van der Zande et al**,)26(silver was eliminated at an extraordinarily slow pace in the brain, which still had significant silver concentrations two months after the final treatment. In another study, even after a 4-month recovery period, silver concentrations in the brain did not return to control levels, demonstrating that silver removal is difficult across biological barriers like the BBB or BTB.

In agreement with these findings, the current study's findings revealed that AgNPs have a degree of tissue toxicity, but that recovery occurs after a period of time.

CONCLUSIONS

Overexposure to AgNPs results in atrophic and degenerative alterations in the tongue's surface epithelium and lamina propria on both the dorsal and ventral surfaces. The surface epithelium, lamina propria, and salivary glands can regenerate and improve their histological image after a one-month recovery period.

RECOMMENDATIONS

Silver nanoparticles should be used with caution, especially in the medical area. AgNPs with a particle size greater than 20nm are strongly suggested, as smaller nanoparticles have been shown to have substantial cytotoxic effects. Further researches are needed to see if a longer recovery period of 2, 3, or 6 months after the discontinuation of AgNPs delivery has a greater protective impact.

REFERENCES

1. Drexler, K. Eric. Engines of Creation: The Coming Era of Nanotechnology. Doubleday. 1986; 5; 82-85.
2. Wijnhoven SW, Peijnenburg WJ, Herberts CA, Hagens WI, Oomen AG, Heugens EH, Roszek B, Bisschops J, Gosens I,Meent D, Dekkers S, De Jong WH, Zijverden M, Sips AJ, Geertsma RE. Nano-silver-a review of available data and knowledge gaps in human and environmental risk assess-ment Nanotox. 2009; 3: 109–138.
3. Madheswaran T, Baskaran R, Yoo BK, Kesharwani P. In vitro and in vivo skin distribution of 5α-reductase inhibitors loaded into liquid crystalline nanoparticles, J Pharm Sci, 2017; 772-782.
4. Allker RP. The use of nanoparticles to control oral biofilm formation. J Dent Res. 2010; 89: 1175-1186.
5. Silva T, Pokhrel LR, Dubey B, Tolaymat TM, Maier KJ, Liu X. Particle size, surface charge and concentration dependent ecotoxicity of three organo-coated silver nanoparticles: Comparison between general linear model-predicted and observed toxicity. Sci Tot Environ. 2014: 968–976.
6. Chen X, Schluesener HJ. Nano-silver: A nanoproduct in medical application. Toxicol Lett. 2008; 16: 1-12
7. Ji JH, Jung JH, Kim SS, Yoon JU, Park JD, Choi BS, Chung YH. Twenty- eight day inhalation toxicity study of silver nanoparticles in Sprague-Dawley rats. Inhal Toxicol. 2007; 19: 857-871.
8. AshaRani PV, Low Kah Mun G, Hande MP, Valiyaveettil S. Cytotoxicity and genotoxicity of silver nanoparticles in human cells. ACS Nano. 2008; 3: 279–290.
9. Wang F, Chen Z, Chunyan M, Lei Bi. Silver Nanoparticles Induce Apoptosis in HepG2 Cells through Particle-Specific Effects on Mitochondria. Environmental Science & Technology. 2022; 56: 5706-5713.
10. Prashant B. Chouke, Ajay K. Manoj M. Rai, Kanhaiya M. Alok R. Rai. Bioinspired NiO Nanospheres: Exploring In Vitro Toxicity Using Bm-17 and L. rohita Liver Cells, DNA Degradation, Docking, and Proposed Vacuolization Mechanism. ACS Omega. 2022; 7: 6869-6884.
11. Li Y, Cummins EJ. Hazard characterization of silver nanoparticles for human exposure routes. Environ Sci Health A Tox Hazard Subst Environ Eng. 2020; 55 :704-725.

12. Lamberti M, Zappavigna S, Sannolo N, Porto S, Caraglia M. Advantages and risks of nanotechnologies in cancer patients and occupationally exposed workers. Expert Opin Drug Deliv. 2014; 11: 1087–1101.

13. Ahmad N, Sharma S, Rai R. Rapid green synthesis of silver and gold nanoparticles using peels of Punica granatum. Adv Mater Lett. 2012; 3: 376-380.

14. Drury RB, Wallington EA. Carleton's histological technique. 5th ed. Oxford, New York, Toronto: Oxford University Press; 1980.

15. Shahare B, Yashpal M. Toxic effects of repeated oral exposure of silver nanoparticles on small intestine mucosa of mice. Toxicol Mech Meth. 2013; 23: 161–167.

16. Sarhan OM, Hussein RM. Effects of intraperitoneally injected silver nanoparticles on histologicalstructures and blood parameters in the albino rat: Int J Nanomed Annual. 2014; 9: 1505-1513.

17. Oberdorster G. Safety assessment for nanotechnology and nanomedicine: concepts of nanotoxicology. J Int Med, 2010; 267: 89-105.

18. AshaRani PV, Mun GL, Hande MP, Valiyaveettil S. Cytotoxicity and genotoxicity of silvernanoparticles in human cells. ACS Nano. 2009; 3: 279–290.

19. Osborne OJ, Johnston BD. Moger J. Balousha M, Lead JR, Kudoh T, Tyler CR. Effects of particle size and coating on nanoscale Ag and TiO(2) exposure in zebrafish (Daniorerio) embryos Nanotox. 2013; 7: 1315-1324.

20. Freed JK, Gutterman DD. Mitochondrial Reactive Oxygen Species and Vascular Function. Arterioscler. Thromb. Vasc. Biol. 2013; 33: 673–675.

21. Cortese-Krott MM, Munchow M, Pirev E, Hessner F, Bozkurt A. silver ions induce oxidative stress and intarcellular zinc release in human skin fibroblast. Free Radic Biol Med. 2009; 47: 1570-157.

22. Cayli S, Ocakli S, Senel U, Eyerci N, Delibasi T. Role of Valosin- containing protein (VCP) and Jab1/CSN5 in testicular ischaemia-reperfusion injury. Mol histol. 2016; 47: 91-100.

23. Cheng X, Zhang W, Ji Y. Revealing silver cytotoxicity using Au nanorods/Ag shell nanostructures: disrupting cell membrane and causing apoptosis through oxidative damage RSC Adv. 2013; 33: 2296-2305.

24. Hussain SM, Javorina AK, Schrand AM, Duhart HM, Ali SF, Schlager JJ. The interaction of manganese nanoparticles with PC-12 cells induces dopamine depletion. Toxicol Sci. 2006; 92: 456–463.

25. Rungby J, Danscher G. Localization of exogenous silver in brain and spinal cord of silver exposed rats. Acta Neuropath. 1983; 60: 92–98.

26. Van der Zande M, Vandebriel RJ, Van Doren E, Kramer E, Herrera Rivera Z, Serrano-Rojero CS, Gremmer ER, Mast J, Peters RJB, Hollman PCH, Hendriksen PJM, Marvin HJP, Peijnenburg AACM, Bouwmeester H. Distribution, elimination, and toxicity of silver nanoparticles and silver ions in rats after 28-day oral exposure. ACS Nano. 2012; 6: 7427–7442.